A GAA repeat expansion reporter model of Friedreich's ataxia recapitulates the genomic context and allows rapid screening of therapeutic compounds

Michele M.P. Lufino[1], Ana M. Silva[1,2], Andrea H. Németh[3,4], Javier Alegre-Abarrategui[1,5], Angela J. Russell[6,7] and Richard Wade-Martins[1,5,*]

[1]Department of Physiology, Anatomy and Genetics, University of Oxford, Le Gros Clark Building, South Parks Road, Oxford OX1 3QX, UK, [2]Faculdade de Medicina, Universidade de Lisboa, Lisboa 1649-028, Portugal, [3]Nuffield Department of Clinical Neurosciences, University of Oxford, Oxford OX3 9DU, UK, [4]Department of Clinical Genetics, Churchill Hospital, Oxford University Hospitals NHS Trust, Oxford OX3 7LE, UK, [5]Oxford Parkinson's Disease Centre, University of Oxford, Le Gros Clark Building, South Parks Road, Oxford OX1 3QX, UK, [6]Department of Chemistry, Chemistry Research Laboratory and [7]Department of Pharmacology, University of Oxford, Mansfield Road, Oxford OX1 3QT, UK

Friedreich's ataxia (FRDA) is caused by large GAA expansions in intron 1 of the frataxin gene (*FXN*), which lead to reduced *FXN* expression through a mechanism not fully understood. Understanding such mechanism is essential for the identification of novel therapies for FRDA and this can be accelerated by the development of cell models which recapitulate the genomic context of the *FXN* locus and allow direct comparison of normal and expanded *FXN* loci with rapid detection of frataxin levels. Here we describe the development of the first GAA-expanded *FXN* genomic DNA reporter model of FRDA. We modified BAC vectors carrying the whole *FXN* genomic DNA locus by inserting the luciferase gene in exon 5a of the *FXN* gene (pBAC-*FXN-Luc*) and replacing the six GAA repeats present in the vector with an ∼310 GAA repeat expansion (pBAC-*FXN-GAA-Luc*). We generated human clonal cell lines carrying the two vectors using site-specific integration to allow direct comparison of normal and expanded *FXN* loci. We demonstrate that the presence of expanded GAA repeats recapitulates the epigenetic modifications and repression of gene expression seen in FRDA. We applied the GAA-expanded reporter model to the screening of a library of novel small molecules and identified one molecule which up-regulates *FXN* expression in FRDA patient primary cells and restores normal histone acetylation around the GAA repeats. These results suggest the potential use of genomic reporter cell models for the study of FRDA and the identification of novel therapies, combining physiologically relevant expression with the advantages of quantitative reporter gene expression.

INTRODUCTION

Friedreich's ataxia (FRDA; OMIM 229300) is a progressive neurodegenerative disorder and the most common form of recessive ataxia, affecting approximately 1–2 in 50 000 Caucasians (1). Patients present with progressive gait and limb ataxia, lower limb areflexia, dysarthria, increased incidence of diabetes and hypertrophic cardiomyopathy, which subsequently leads to death in the fourth or fifth decade of life (2,3). The neurological symptoms are mainly caused by degeneration of the large sensory neurons of the dorsal root ganglia, the spinocerebellar tracts and the dentate nucleus of the cerebellum (4,5). FRDA is caused by an abnormal expansion of GAA repeats in intron 1 of the frataxin gene (*FXN*) (1). Approximately 98% of FRDA patients are homozygous for a GAA repeat expansion and the remaining patients are compound heterozygous with one

*To whom correspondence should be addressed. Tel: +44 1865282837; Fax: +44 1865272420; Email: richard.wade-martins@dpag.ox.ac.uk

expanded allele and a point mutation in the second allele (6,7). Normal unaffected individuals have <36 GAA repeats, whereas FRDA patients present with GAA expansions ranging from 70 to >1000 GAA repeats which lead to reduced levels of frataxin, a nuclear-encoded mitochondrial protein essential for life (1,8). The GAA size of the small allele has been shown to correlate with residual frataxin levels, earlier onset and increased severity of disease (9,10). Frataxin deficiency leads to iron–sulphur cluster deficiency, mitochondrial iron accumulation and increased susceptibility to oxidative stress (11–16).

The mechanism through which expanded GAA repeats silence *FXN* expression still needs further elucidation. Two non-exclusive models have been proposed (11,17). Initial evidence suggested that expanded GAA repeats in intron 1 of *FXN* form unusual DNA structures such as triplexes or sticky DNA and DNA/RNA hybrid structures, which impede the progress of the RNA polymerase and perturb transcription in a length-dependent manner (18–24). However, more recently, a second model suggests that long GAA expansions can induce silencing of *FXN* expression via a heterochromatin-mediated mechanism of repression (25,26). Epigenetic changes around expanded GAA repeats have been identified, which include increased DNA methylation at specific CpG sites upstream of the GAA repeats (27–30) and reduced acetylation of histones H3 and H4 accompanied by increased levels of methylated histones H3K9me2 and H3K9me3 in regions flanking GAA repeats (26,31). The *FXN* promoter in patient-derived cells and tissues shows a less permissive configuration for transcription initiation (27,32). More recently, a depletion of chromatin insulator protein CTCF was identified at the *FXN* promoter of FRDA patient-derived cells and a correlation between CTCF depletion and increased levels of the frataxin antisense transcript-1 was suggested (33).

Currently, there is no proven treatment for FRDA, although there are promising therapies under development (26,34–37). A better understanding of the *FXN* silencing which occurs in the presence of large GAA expansions is vital for the identification of novel therapies for FRDA. The development of reporter models which reproduce the epigenetic hallmarks of FRDA while providing efficient ways to quantify *FXN* expression would considerably accelerate the identification of such treatments. A few GAA-based reporter models have been described; however, these focus only on the use of short heterologous reporter constructs carrying expanded GAA repeats out of context and lacking *FXN* genomic DNA sequences (31,38,39). Such models do not carry repeat expansions within the *FXN* locus and thus they do not allow the analysis of the nature of the *FXN* silencing induced by long GAA repeats. A reporter model based on the use of the whole *FXN* genomic DNA locus would provide instead an excellent tool for such study since the expansion would be present within its natural genomic context, within intron 1 of the *FXN* gene. Furthermore, such reporter models achieve physiologically relevant *FXN* expression, since the native promoter and all the regulatory elements necessary for physiological gene expression are present in the vector (40–42).

Here we describe the development and characterization of the first GAA-expanded genomic DNA reporter model of FRDA. Using homologous recombination, we modified a BAC carrying the 80 kb *FXN* locus by inserting the reporter gene luciferase in exon 5a of the *FXN* gene, generating the pBAC-*FXN-Luc* vector. We also replaced a normal number of GAA repeats (six

GAA) present in pBAC-*FXN-Luc* with ∼310 GAA repeats (pBAC-*FXN-GAA-Luc* vector) and generated stable clonal cell lines in order to compare the effect of normal or expanded GAA repeats on the *FXN* gene. Using site-specific integration coupled with a copy number assay, we generated highly comparable cell lines which allow comparison in the absence of confounding effects. We show that ∼310 GAA repeats decrease *FXN* expression by greatly affecting the epigenetic landscape of the *FXN* locus. Finally, we applied this novel reporter model to the screening of a library of small molecules and identified a molecule which up-regulates *FXN* expression in FRDA patient cells and reverses the GAA-induced *FXN* gene silencing by increasing histone acetylation at the *FXN* locus. We believe that our genomic DNA reporter model allows accurate comparison of normal and GAA-expanded *FXN* loci within a physiological genomic context and provides a tool for rapid and cost-effective identification of *FXN* up-regulating therapeutic strategies.

RESULTS

Construction of pBAC-*FXN-Luc* and pBAC-*FXN-GAA-Luc* genomic DNA reporter vectors

A BAC clone (RP11-265B8) containing the whole *FXN* locus from human chromosome 9 was used to generate *FXN-Luc* BAC vectors. This vector contains approximately 38 kb of promoter region, the 80 kb *FXN* locus and 17 kb of downstream sequence (42). Since the most abundant *FXN* transcript consists of exons 1–5a (1,43), we inserted the firefly luciferase sequence in exon 5a immediately prior to the stop codon, generating pBAC-*FXN-Luc* fusion vector (Fig. 1A). We included a sequence encoding a five amino-acid Gly-Ser-Gly-Ser-Gly (GSGSG) peptide linker between the exon 5a and luciferase sequence (Fig. 1A) to allow correct folding of the frataxin and luciferase proteins; the choice of the composition of the linker was based on previous reports (44). Construction of pBAC-*FXN-Luc* was achieved by a selection/counter-selection homologous recombination strategy using homology arms to exon 5a. To confirm correct vector recombination, successful colonies were analysed by junction PCR, by restriction enzyme digestion followed by pulsed-field gel electrophoresis (PFGE) and by sequencing, which confirmed correct insertion of the GSGSG-luciferase sequence in exon 5a (data not shown). The resulting modified *FXN* gene expresses an FXN-luciferase fusion protein within the context of the *FXN* genomic DNA locus.

In order to insert a GAA expansion into intron 1 of the pBAC-*FXN-Luc* vector, a PCR product containing expanded GAA repeats was amplified from genomic DNA isolated from an FRDA patient-derived lymphoblastoid cell line (GM16207, alleles with 280 and 830 GAA repeats in the *FXN* gene) using an established PCR protocol (1,45). The smaller PCR product carrying ∼280 GAA repeats flanked by 195 and 255 bp of homology arms upstream and downstream of the GAA repeats, respectively, was preferentially amplified and used for recombination. We used the RPSL-Neo selection/counter-selection homologous recombination method to replace the six GAA repeats present in the *FXN*-BAC in intron 1 of *FXN-Luc* gene with the expanded GAA repeats amplified by PCR, generating pBAC-*FXN-GAA-Luc* vector. Owing to low efficiency of recombination, successful colonies were identified through
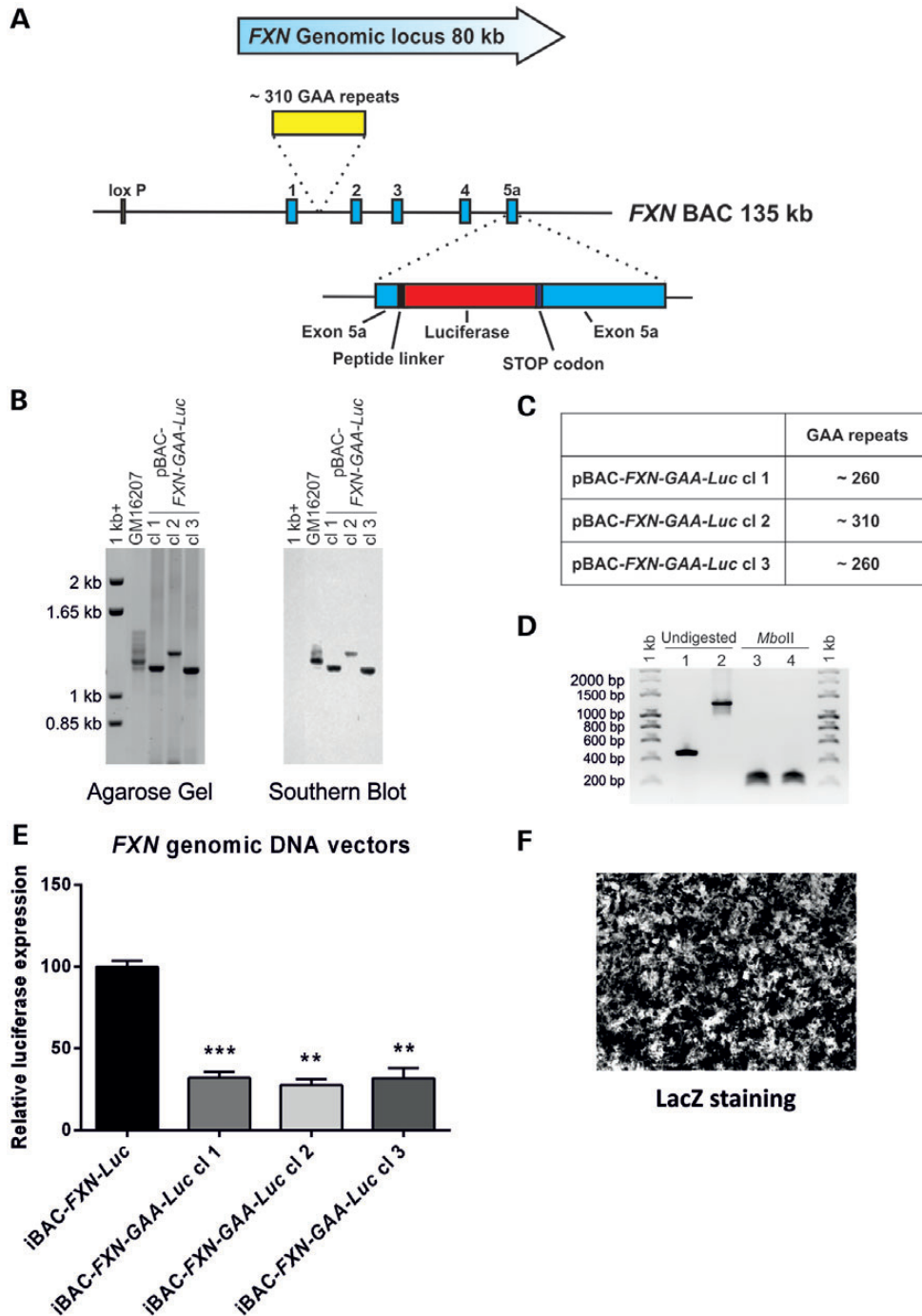
Figure 1. Generation of pBAC-*FXN-Luc* and pBAC-*FXN-GAA-Luc* genomic DNA reporter vectors. (**A**) Schematic representation of the construction of pBAC-*FXN-Luc* and pBAC-*FXN-GAA-Luc* vectors. Construction was achieved in two successive rounds of selection–counter-selection homologous recombination. First, a luciferase sequence preceded by a GSGSG peptide linker was introduced at the 5′ end of exon 5a, immediately before the stop codon, generating pBAC-*FXN-Luc* vector. This vector expresses an FXN-luciferase fusion protein and carries six GAA repeats in intron 1. To generate pBAC-*FXN-GAA-Luc* vector, a second recombination was performed to replace the six GAA repeats present in intron 1 with ∼310 GAA repeats amplified from FRDA patient-derived cells. (**B**) Successful insertion of expanded GAA repeats was confirmed by Southern blot by using a DIG-labelled TTC$_{10}$ probe. Comparison with ladder allowed sizing of GAA repeats as reported in (**C**). (C) Size of GAA expansions in pBAC-*FXN-GAA-Luc* clones. (**D**) pBAC-*FXN-GAA-Luc* cl 2 vector carries ∼310 pure GAA repeats. GAA repeats were amplified from pBAC-*FXN-Luc* (lane 1) and pBAC-*FXN-GAA-Luc* (lane 2) vectors, incubated with *Mbo*II and run on a 1% agarose gel. The PCR products of pBAC-*FXN-Luc* (lane 3) and pBAC-*FXN-GAA-Luc* (lane 4) are fully digested by the enzyme, leaving the flanking regions of 208 and 248 bp and demonstrating the lack of interruptions in the GAA expansion. (**E**) To assess whether expanded GAA repeats reduce FXN-luciferase expression, we delivered iBAC-*FXN-Luc* and iBAC-*FXN-GAA-Luc* vectors to the neuronal cell line SH-SY5Y using HSV-1 amplicon vectors. Luciferase assay showed a 70–75% reduction in FXN-luciferase levels in the three iBAC-*FXN-GAA-Luc* clones. Error bars represent mean ± SEM ($n = 3$). **$P < 0.01$, ***$P < 0.001$ as determined by the one-way ANOVA compared with iBAC-*FXN-Luc*, with Dunnett's test. (**F**) LacZ staining of the experiment described in (E) shows high efficiency of vector delivery to SH-SY5Y cells.

colony blot using a TTC$_{10}$ probe. The GAA expansion of three independent colonies was sized through Southern blotting, which confirmed an insertion of up to ∼310 GAA repeats (Fig. 1B and C). To assess the purity of the ∼310 GAA repeats, sequencing was performed from both sides. We confirmed the presence of 213 GAA repeats on the GAA strand and 125 GAA repeats on the TTC strand, thereby achieving an overlap of at least 28 GAA repeats (data not shown). The presence of such overlap ensured that the whole GAA expansion was sequenced. We detected no interruptions in the expanded GAA sequence and this was further corroborated by *Mbo*II digestion according to a method previously described (Fig. 1D) (46). The GAA repeats were amplified from pBAC-*FXN-GAA-Luc* cl 2 vector by PCR and digested with *Mbo*II. The complete digestion of the PCR product confirms the purity of the GAA expansion in the pBAC-*FXN-GAA-Luc* cl 2 vector (Fig. 1D).

Validation of pBAC-*FXN-Luc* and pBAC-*FXN-GAA-Luc* reporter constructs

To investigate the effect of ∼310 GAA repeats on FXN-luciferase expression in the human neuronal cell line SH-SY5Y, we used the herpes simplex virus type-1 (HSV-1) amplicon vector system. SH-SY5Y cells are characterized by low efficiency of transfection and HSV-1 vectors mediate intact delivery of BACs to cells at high efficiency (40,47). To allow packaging into HSV-1 amplicons, we used *Cre/loxP* recombination (Fig. 2A) to incorporate into pBAC-*FXN-Luc* and pBAC-*FXN-GAA-Luc* a retrofitting vector containing the HSV-1 *oriS* origin of replication and *pac* packaging signals, a *lacZ* cassette for titration and sequences derived from the Epstein–Barr virus for extra-chromosomal vector retention, generating iBAC-*FXN-Luc* and iBAC-*FXN-GAA-Luc*, respectively. Correctly retrofitted vectors were identified using PFGE analysis, and vectors were packaged into HSV-1 amplicons using an improved helper virus-free packaging protocol as described previously (data not shown) (48). Average titres of $1-2 \times 10^7$ transducing units per millilitre were obtained for all vectors. SH-SY5Y cells were transduced with iBAC-*FXN-Luc* and iBAC-*FXN-GAA-Luc* cl 1, 2 and 3 amplicons at a multiplicity of infection of 4 and luciferase assay was performed 4 days after infection. High efficiency of transduction was achieved as determined by LacZ staining (Fig. 1F). The presence of up to ∼310 GAA repeats in iBAC-*FXN-GAA-Luc* vectors causes a reduction in FXN-luciferase expression by ∼75% when compared with iBAC-*FXN-Luc* vector, recapitulating the effect of GAA repeats on *FXN* expression observed in FRDA patient cells (Fig. 1E). pBAC-*FXN-GAA-Luc* cl 2 vector (referred to as pBAC-*FXN-GAA-Luc*) was chosen for the following experiments.

Generation and characterization of a GAA-expanded genomic DNA reporter model of FRDA

In order to generate a cell model which allows the dissection of the effect of GAA repeats on *FXN* expression, we generated stable clonal cell lines carrying pBAC-*FXN-Luc* and pBAC-*FXN-GAA-Luc* vectors by using site-specific vector integration, since random vector integration in the genome can affect

transgene expression levels. Site-specific integration allows precise comparison of the two vectors in the absence of confounding effects due to differential integration site, since the two vectors are integrated at the same genomic location. To generate these cell lines, we adapted the previously described Flp-In system (Life Technologies) to BAC vectors. We developed an Flp-In BAC integration system by generating the retrofitting vector pH-FRT-Hy (Fig. 2A), which contains the Flp-In promoter-less hygromycin cassette. pH-FRT-Hy was then retrofitted into the pBAC-*FXN-Luc* and pBAC-*FXN-GAA-Luc* vectors using the *Cre/loxP* retrofitting strategy previously described (40), generating pFRT-*FXN-Luc* and pFRT-*FXN-GAA-Luc* vectors (Fig. 2A). A stable FRT acceptor cell line was generated by transfecting HEK cells with the plasmid pFRT-LacZeo, followed by zeocin selection and confirmation of positive LacZ staining (HEK FRT cells). These cells were transfected with pFRT-*FXN-Luc* and pFRT-*FXN-GAA-Luc* vectors together with the Flp recombinase-encoding plasmid pOG44 (Life Technologies). Stable clonal cell lines (referred to as *FXN-Luc* and *FXN-GAA-Luc*) were isolated in the presence of hygromycin, and PCR was used to confirm correct vector integration at the FRT acceptor site (Fig. 2B). Random integration events are prevented since the promoter which drives hygromycin is only present at the docking site and any integration at other genomic locations will not result in antibiotic resistance. The presence of GAA repeats in *FXN-GAA-Luc* cells was confirmed by PCR (data not shown). Clonal cell lines were expanded and characterized.

Fluorescence *in situ* hybridization (FISH) was performed on *FXN-Luc* and *FXN-GAA-Luc* clonal cell lines using the unmodified *FXN* BAC and the pH-FRT-Hy retrofitting vector as probes which, when co-localizing, indicate the presence of the integrated vector (Fig. 2C). *FXN-Luc* and *FXN-GAA-Luc* cell lines, which have been generated using different vectors, both show vector integration at the same location, on chromosome 1p as confirmed by the use of a chromosome 1 centromeric probe (data not shown), confirming the consistency of the site-specific integration for large genomic DNA vectors (Fig. 2C). We then assessed vector copy number in *FXN-Luc* and *FXN-GAA-Luc* cells by real-time PCR, using as reference sample the acceptor cell line HEK FRT, which carries three endogenous *FXN* loci as determined by FISH (Fig. 2C). We used this assay to select *FXN-Luc* and *FXN-GAA-Luc* clonal cell lines carrying one copy of transgene (Fig. 2D).

We then determined the effect of the GAA repeat expansion on FXN-luciferase expression by reverse transcription real-time PCR (qRT-PCR) and by luciferase assay. The presence of GAA repeats causes a reduction of 37% in FXN-luciferase mRNA levels (Fig. 2F) and 42% in FXN-luciferase protein levels (Fig. 2G), as determined by qRT-PCR and by luciferase assay, respectively. Western blot analysis shows that *FXN-Luc* and *FXN-GAA-Luc* cells express an FXN-luciferase fusion protein of the expected size of ∼79 kDa (Fig. 2E).

Epigenetic characterization of *FXN-Luc* and *FXN-GAA-Luc* cell lines

Recently, it has been shown that the presence of GAA repeats in intron 1 of the *FXN* locus reduces *FXN* expression by heterochromatin formation and increased CpG methylation around GAA
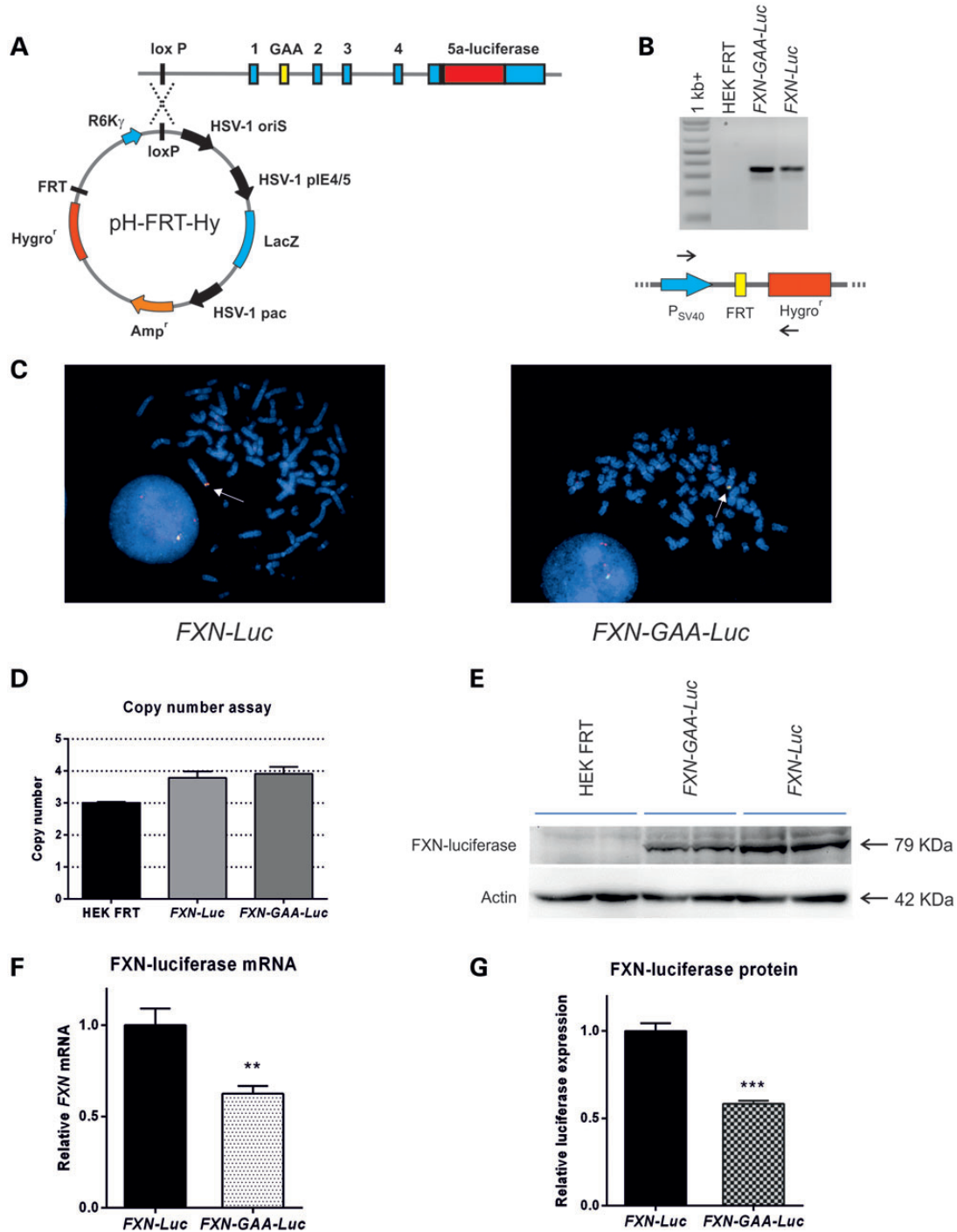
Figure 2. Generation and characterization of a GAA-expanded genomic DNA reporter model of FRDA. (**A**) Schematic representation of *Cre/loxP* retrofitting of pBAC-*FXN-Luc* and pBAC-*FXN-GAA-Luc* vectors with pH-FRT-Hy. pH-FRT-Hy carries a promoter-less hygromycin cassette preceded by an FRT site. (**B**) Site-specific vector integration in *FXN-Luc* and *FXN-GAA-Luc* cells is confirmed by PCR using primers targeting the P_{SV40} promoter and the hygromycin cassette. (**C**) FISH analysis was performed on a representative clonal cell line for each vector, using the unmodified *FXN*-BAC (red) and the retrofitting vector pH-FRT-Hy (green) as probes. Co-localization of the two probes (arrows) shows vector integration in chromosome 1p. Chromosome identity was confirmed using a chromosome 1 centromeric probe (data not shown). The cells analysed here carry three copies of the endogenous *FXN* locus, due to the hypotriploid nature of HEK cells. (**D**) Copy number was used to identify stable cell lines with one vector copy. Copy number was determined by real-time PCR using UpGAA primers and data normalized by *GAPDH*. Data are expressed as relative to HEK FRT, which was set to three copies based on the identification in (C) of three endogenous *FXN* loci. (**E**) Western blot analysis of *FXN-Luc* and *FXN-GAA-Luc* clonal cell lines using an anti-luciferase antibody shows a ∼79 kDa band which corresponds to the expected size for the FXN-luciferase fusion protein. (**F**) qRT-PCR in *FXN-Luc* and *FXN-GAA-Luc* clonal cell lines using exon 5a-Luc primers shows a 37% reduction in FXN-luciferase mRNA levels in *FXN-GAA-Luc* cells. Exon 5a-Luc data are normalized to *GAPDH* and expressed as relative to *FXN-Luc* cells. Error bars represent mean ± SEM ($n = 4$). **$P < 0.01$, as determined by Student's *t*-test. (**G**) Luciferase assay shows a 42% reduction in FXN-luciferase protein levels. Data are expressed as relative light units and normalized to total cell protein. Error bars represent mean ± SEM ($n = 3$). ***$P < 0.001$, as determined by Student's *t*-test.

repeats (26,27). To test for the presence of repressive epigenetic hallmarks in our cell model, we first analyzed histone modifications by chromatin immunoprecipitation (ChIP) at three sites, at the promoter and the regions flanking GAA repeats, upstream and downstream of GAA repeats, using antibodies specific for the human acetylated histones H3K9 and H4K8 and di- and tri-methylated histone H3K9. This analysis revealed a decrease in histone acetylation and an increase in histone methylation across the three regions in the *FXN-GAA-Luc* cell line when compared with *FXN-Luc* cells (Fig. 3A), as previously reported in FRDA patient brain tissue and patient-derived cell lines (26,27,32).

We then analyzed CpG methylation by bisulfite sequencing as reported in previous studies (27). In the region upstream of the expanded GAA repeats, we found increased DNA methylation in *FXN-GAA-Luc* cells at CpG sites 4 and 5 (Fig. 3B), in agreement with previously published methylation data from FRDA patients (27,29). Our results for CpG 6 differ from the results previously found in patients (27,28), but are in agreement with methylation data from the brain of FRDA mice (27). In the region downstream of the GAA repeats, we observed increased DNA methylation at CpG sites 1, 2 and 7 (Fig. 3B).

Since *FXN-Luc* and *FXN-GAA-Luc* cell lines share the same integration site and only differ by the presence of an ~310 GAA repeats expansion, it is most likely that the GAA expansion is causing the changes in histone acetylation/methylation and DNA methylation observed (Fig. 3).

Use of *FXN-GAA-Luc* cell line for the screening of chemical libraries

We have shown above that *FXN-GAA-Luc* cells carry a GAA expansion which causes heterochromatin-mediated silencing of FXN-luciferase expression. Since recent publications report
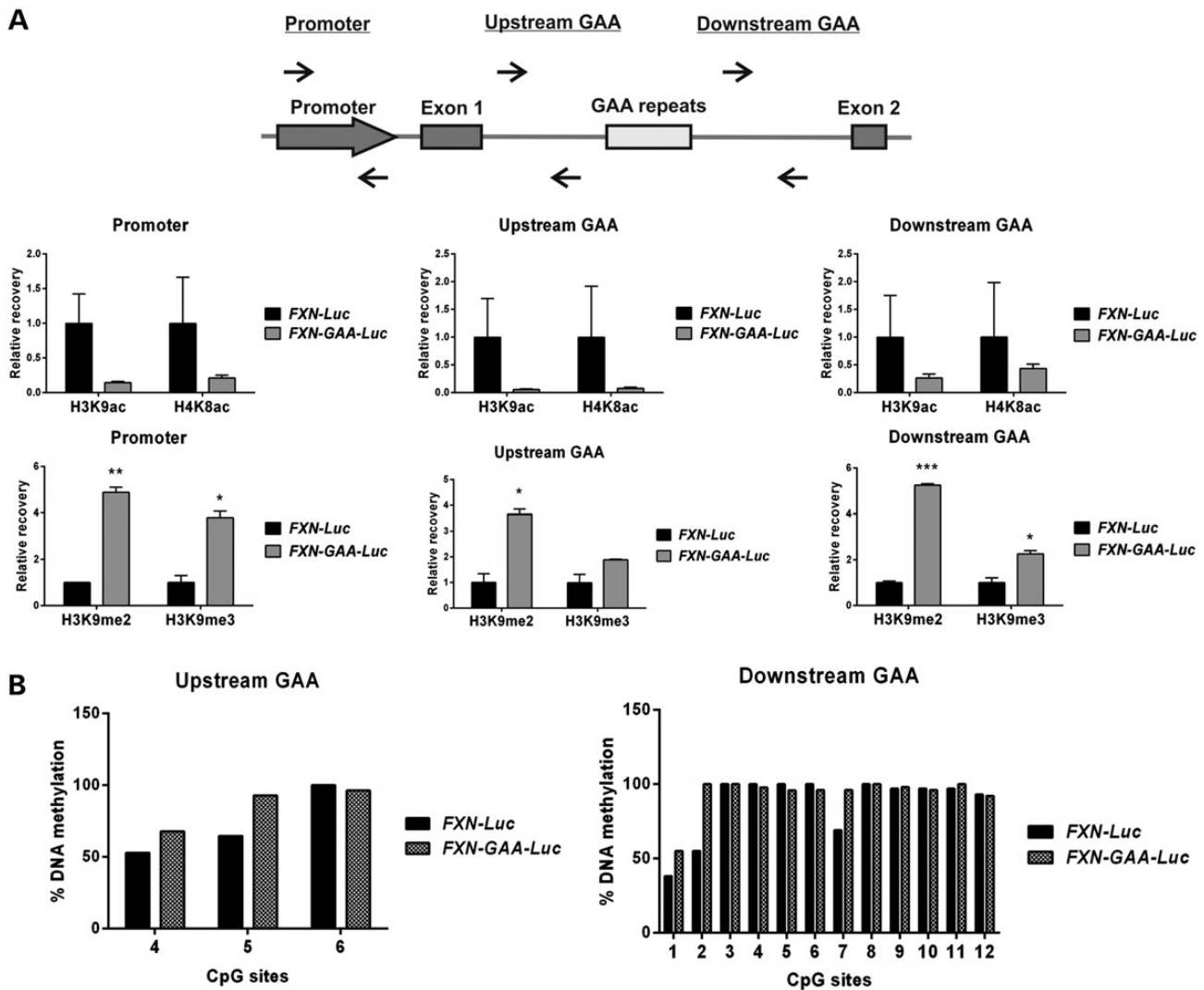

Figure 3. Expanded GAA repeats induce heterochromatin-mediated *FXN* silencing. (**A**) ChIP was performed on *FXN-Luc* and *FXN-GAA-Luc* cells using antibodies specific for the human acetylated histones H3K9 and H4K8 and di- and tri-methylated histone H3K9. The schematic diagram shows the position of the primers used. Error bars represent mean $\pm$ SEM from two independent immunoprecipitations and each immunoprecipitation quantified in triplicate. *$P < 0.05$, **$P < 0.01$, ***$P < 0.001$ as determined by Student's *t*-test. (**B**) CpG methylation was analysed upstream and downstream of GAA repeats using bisulfite sequencing. We found increased DNA methylation at CpG sites 4 and 5 upstream of GAA repeats and at CpG sites 1, 2 and 7 downstream of GAA repeats. A total of 10 colonies were sequenced per region and for each cell line.

the successful up-regulation of *FXN* expression with histone deacetylase (HDAC) inhibitors (26,34), we applied our novel genomic DNA reporter model of FRDA to the screening of novel small molecules with potential HDAC inhibitor function. We screened *in silico* a library of 25 000 compounds to extract representative structures incorporating known pharmacophores associated with HDAC inhibitors and, more generally, with Zn(II)-binding motifs. This library has been designed to cover a wide range of biological space, including pharmacophores with well-characterized biological mechanisms in addition to structural motifs which exhibit biological effects with an unknown mechanism (49,50). Structures have been excluded which contain highly reactive functionalities (e.g. aldehydes, or Schiff bases) or known toxicophores (e.g. poly-halogenated species or poly-nitro aromatics) and selected structures are amenable to both resynthesis and rapid diversification. Compounds were selected from this library based on the presence of motifs likely to bind to Zn(II), such as hydroxamic acids, diamines and amino alcohols, which may plausibly inhibit zinc-dependent enzymes such as HDACs. However, alternative mechanisms of action cannot be ruled out. We identified 88 potential Zn(II)-binding compounds and performed the screening of such molecules in a 96-well format in triplicate by incubating *FXN-GAA-Luc* cells at a standard concentration of 20 μM for 48 h and assessing FXN-luciferase expression by luciferase assay (Fig. 4A). We identified four compounds which significantly increased *FXN-GAA-Luc* expression levels above dimethyl sulphoxide (DMSO) levels. In order to exclude the possibility of interaction of compounds with the luciferase

assay and to discard those that show a generalized unspecific increase of gene expression, we tested the effect of the selected four compounds on luciferase expression driven by the ubiquitous cytomegalovirus (CMV) promoter (Fig. 4B). None of the four compounds shows an increase in luciferase expression; however, three compounds show a decrease in luciferase levels, which could indicate early signs of cell toxicity. To avoid potentially cytotoxic molecules, we focused subsequent studies on compound C5, the only molecule which did not affect CMV-luciferase levels (Fig. 4B).

To assess whether C5 acts as an HDAC inhibitor on the *FXN* gene and is able to reverse the GAA-mediated *FXN* silencing, we incubated FRDA patient lymphoblastoid cells with C5 at 20 μM for 48 h and analysed H3K9 and H4K8 acetylation upstream and downstream of GAA repeats. The FRDA cell line GM15850 shows a reduction in histone acetylation at these areas when compared with the wild-type cell line GM15851. When FRDA patient cells are incubated with C5, the FRDA histone acetylation is restored to wild-type levels, suggesting C5 acts either directly or indirectly in inhibiting HDAC activity (Fig. 4C). C5 is an amino alcohol and its structure is shown in Figure 4D. To confirm the activity of C5, we sourced an authentic sample and further corroborated its identity through mass spectrometry.

Characterization of C5 on *FXN* expression

In order to further characterize this novel compound, we then performed a dose–response assay by incubating *FXN-GAA-Luc* cells
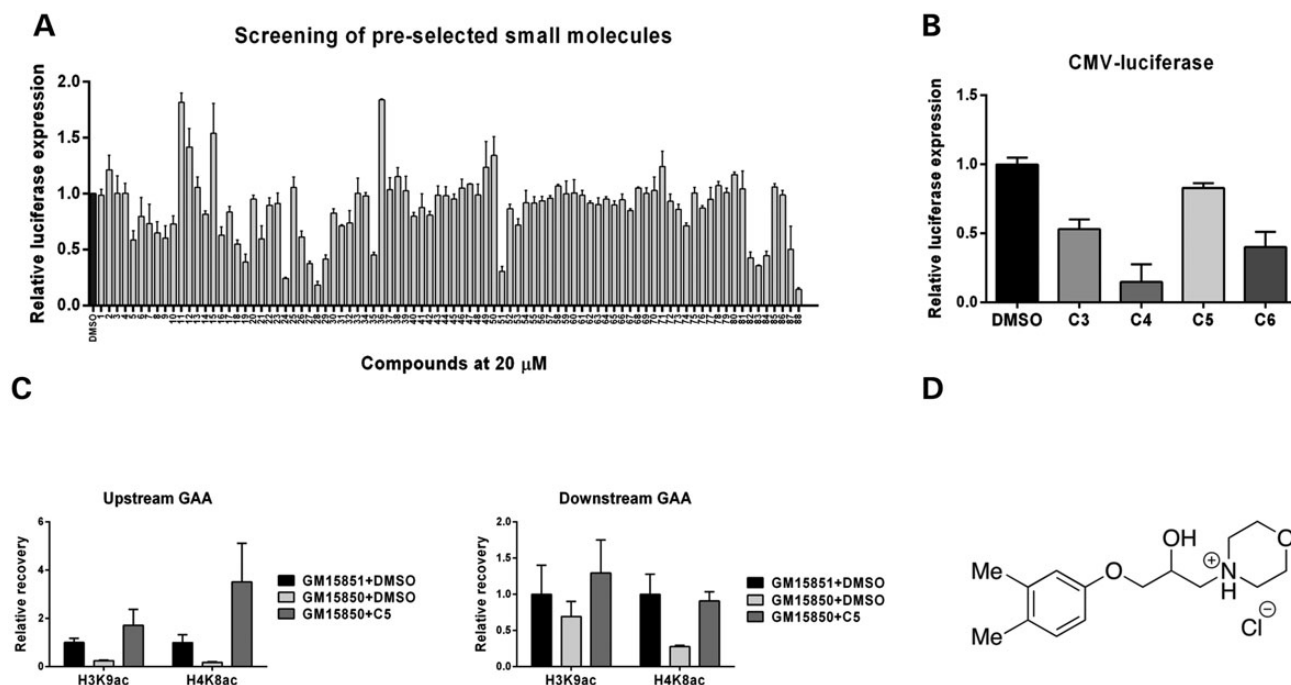

Figure 4. Screening of 88 pre-selected small molecules. (**A**) *FXN-GAA-Luc* cells were incubated in a 96-well format for 48 h with each compound at a final concentration of 20 μM. FXN-luciferase levels were quantified through luciferase assay. Each compound was tested in triplicate. (**B**) Four compounds identified from the screen were tested on HEK cells transfected with a CMV-luciferase plasmid to exclude molecules which directly affect the reporter assay or cause unspecific increase of expression. Transfected cells were incubated with each compound at a concentration of 20 μM for 48 h, followed by luciferase assay. (**C**) C5 increases H3K9 and H4K8 histone acetylation in FRDA lymphoblastoid cells (GM15850) to the normal levels observed in control cells (GM15851). Cells were incubated with C5 at 20 μM for 48 h and ChIP was performed using antibodies specific for the H3K9ac and H4K8ac residues. Error bars represent mean ± SEM from three independent immunoprecipitations and each immunoprecipitation quantified in triplicate. (**D**) Structure of the amino alcohol C5.

with C5 at concentrations ranging from 1 μM to 1 mM for 48 h. A sigmoidal-shaped dose-dependent increase in *FXN-GAA-Luc* expression was observed, with a high up-regulating effect observed at 300, 600 and 1000 μM (Fig. 5A). These three doses were chosen for further studies.

In order to determine whether the increase in *FXN-GAA-Luc* expression is due to an increase in transcription, we incubated *FXN-GAA-Luc* cells with C5 at the three chosen concentrations and analysed *FXN-GAA-Luc* mRNA by qRT-PCR. We show that C5 significantly increases *FXN-GAA-Luc* mRNA levels at 600 and 1000 μM (Fig. 5B). We then compared the effect of C5 on normal and GAA-expanded *FXN* loci, by incubation of *FXN-Luc* and *FXN-GAA-Luc* cells with C5 for 48 h followed by luciferase assay. We found that C5 induces a significantly greater up-regulating effect on the *FXN-GAA-Luc* cells, demonstrating a relative specificity for the expanded *FXN* locus (Fig. 5C). However, a small but significant increase was also observed on *FXN-Luc* cells.

Finally, to exclude a specific action of C5 on the transgene only, we incubated untransfected HEK cells with C5 at the three concentrations for 48 h and quantified endogenous *FXN* mRNA levels. We observed a 1.5–2-fold increase in endogenous *FXN* mRNA at 600 and 1000 μM (Fig. 5D). Furthermore, C5 significantly increases endogenous frataxin protein levels by 1.2-fold at 600 μM and by 1.7-fold at 1000 μM, as determined by frataxin dipstick assay (Fig. 5E).

Validation of C5 in primary cells from FRDA patients

To test the efficacy of C5 as a potential novel therapeutic molecule for FRDA, we tested C5 on primary lymphocytes isolated from FRDA patients, as these cells provide a readily obtainable source of patient primary cells. Primary lymphocytes were isolated from blood samples from three patients, using the Ficoll-Paque gradient as previously described (51). We incubated isolated primary lymphocytes with C5 at concentrations ranging from 300 to 800 μM and after 72 h analyzed *FXN* mRNA levels by qRT-PCR. In order to reduce the influence of fluctuations of reference genes on the final data, we normalized the *FXN* mRNA levels by the geometric mean of three different reference genes. Incubation with C5 up-regulates *FXN* expression in all three patients by 1.5–2-fold (Fig. 6), an increase similar to that observed in *FXN-GAA-Luc* cells. The identification of a new molecule through our cell model and the confirmation of its effect in primary lymphocytes from FRDA patients highlight the suitability of the *FXN-GAA-Luc* cells as a high-throughput expression model of FRDA.

DISCUSSION

Here we describe the generation of a novel genomic DNA reporter model of FRDA which allows direct comparison between normal and GAA-expanded genomic DNA loci and provides
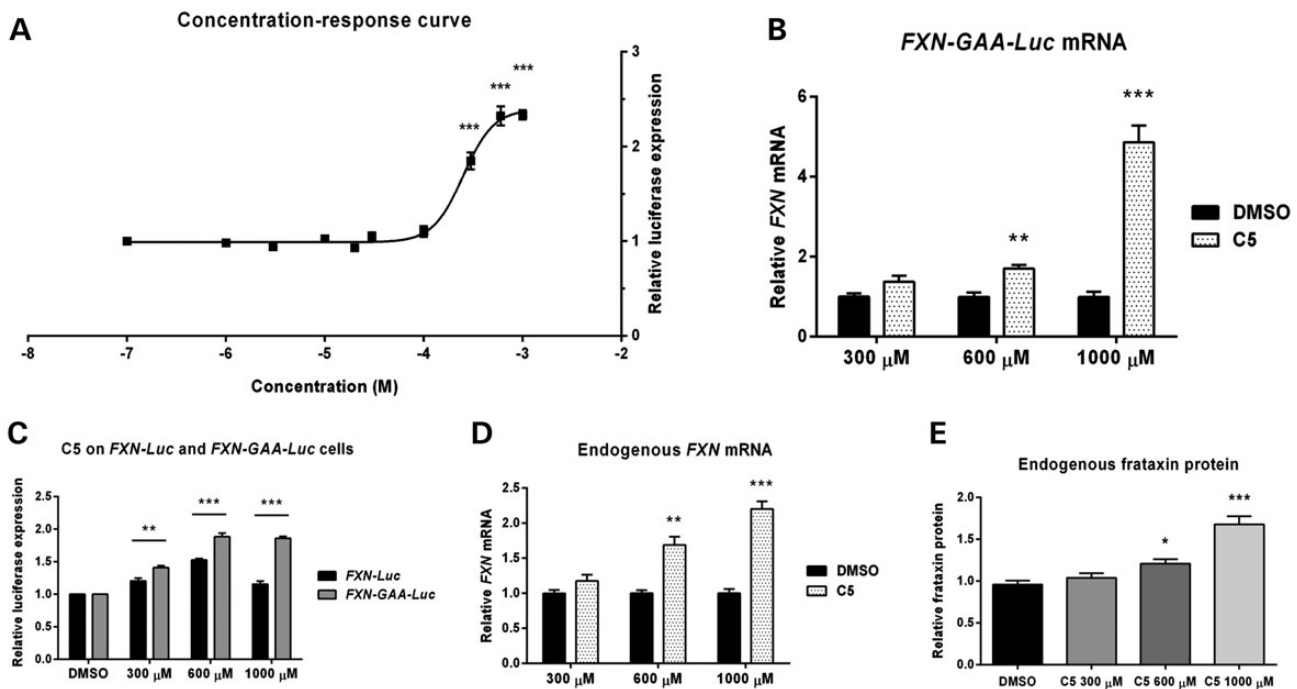

Figure 5. Effect of C5 on *FXN* expression in HEK cells. (**A**) Dose response of C5 on *FXN-GAA-Luc* cells. *FXN-GAA-Luc* cells were incubated for 48 h and luciferase assay was carried out. We identified 300, 600 and 1000 μM as the doses achieving the highest increase in FXN-luciferase expression. Error bars represent mean ± SEM ($n = 3$). ***$P < 0.001$ as determined by the one-way ANOVA compared with DMSO, with Dunnett's test. (**B**) qRT-PCR on *FXN-GAA-Luc* cells incubated with C5 at the three concentrations for 48 h shows a significant increase in *FXN-GAA-Luc* mRNA levels at 600 and 1000 μM. Data are normalized to *GAPDH* mRNA levels. (**C**) Luciferase assay on *FXN-Luc* and *FXN-GAA-Luc* cells after 48 h incubation with C5 at 300, 600 and 1000 μM. C5 shows a greater up-regulation on *FXN-GAA-Luc* cells at all three concentrations, although a smaller but significant increase in *FXN-Luc* cells is also observed. Data for each cell line are normalized by their respective DMSO. (**D**) qRT-PCR on HEK cells incubated with C5 for 48 h shows that C5 is active on the *FXN* endogenous locus. (**E**) C5 significantly increases endogenous frataxin protein levels by 1.2-fold at 600 μM and by 1.7-fold at 1000 μM as determined by frataxin dipstick assay. In (B)–(E), error bars represent mean ± SEM. *$P < 0.05$, **$P < 0.01$, ***$P < 0.001$ as determined by Student's *t*-test (B)–(D) and by the one-way ANOVA compared with DMSO, with Dunnett's test (E).
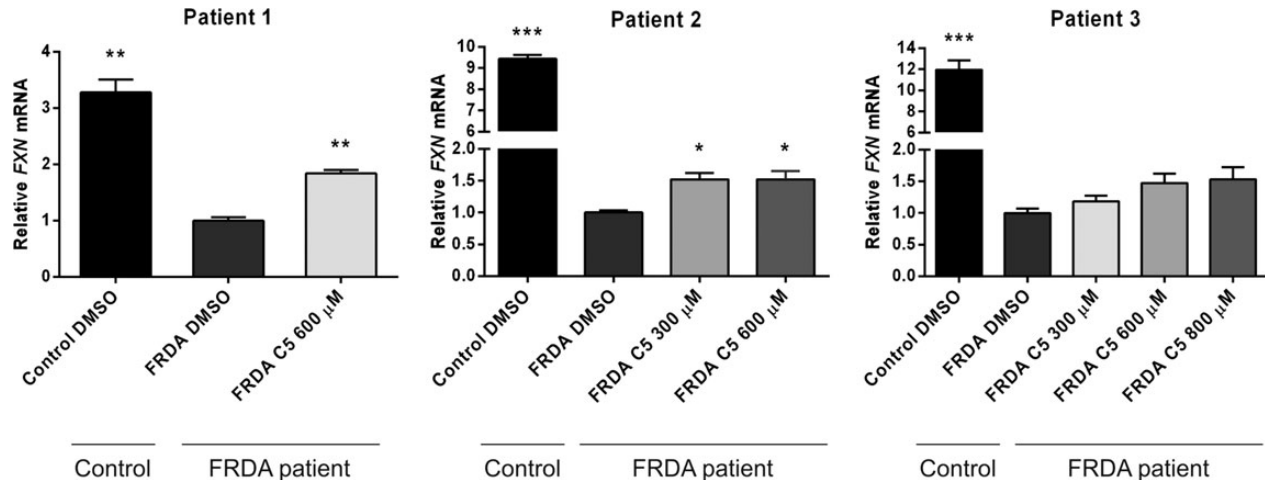
Figure 6. Validation of C5 on primary lymphocytes from FRDA patients. FRDA patient primary lymphocytes were extracted from blood using a Ficoll-Paque gradient and incubated with C5 for 72 h at different concentrations. C5 significantly increases *FXN* expression in patient 1 and 2 and shows a dose-dependent trend in patient 3. *FXN* data are normalized by the geometric mean of three reference genes: *GAPDH*, *HPRT* and *Beta-Actin*. Error bars represent mean $\pm$ SEM ($n = 4$). $^*P < 0.05$, $^{**}P < 0.01$, $^{***}P < 0.001$ as determined by the one-way ANOVA compared with FRDA DMSO, with Dunnett's test.

rapid and precise quantitation of *FXN* expression. To generate this reporter model, we used BAC vectors carrying the whole 80 kb genomic DNA *FXN* locus, since BAC vectors provide a suitable tool to study the molecular behaviour of expanded GAA repeats within their natural genomic context.

We have previously shown the importance of driving transgene expression from the native *FXN* promoter instead of from strong heterologous promoters (52) and we have demonstrated that by delivering a BAC clone (RP11-265B8) containing the whole 80 kb *FXN* locus to FRDA patient primary fibroblasts, we could rescue the increased sensitivity to oxidative stress of such cells to wild-type levels (42). Thus, we used the same BAC clone to create an *FXN* genomic reporter system by inserting a luciferase sequence in exon 5a of *FXN*, generating pBAC-*FXN-Luc* vector. This was performed using a selection/counter-selection homologous recombination protocol based on RecET recombination, which allows precise modification of BAC vectors without leaving behind unwanted sequences such as bacterial antibiotic resistance cassettes, which can affect gene expression (53). pBAC-*FXN-Luc* vector encodes an FXN-luciferase fusion protein of the size of $\sim$79 kDa expressed under the *FXN* native promoter, combining all the advantages of a reporter system with the physiologically relevant expression levels obtained by using the full *FXN* genomic DNA locus. pBAC-*FXN-Luc* vector carries normal allele GAA repeats (six GAA) in intron 1; hence, we replaced these six GAA repeats with an $\sim$310 GAA repeat expansion generating pBAC-*FXN-GAA-Luc*. We demonstrate by sequencing and *Mbo*II digestion that the GAA expansion consists of pure GAA repeats and does not contain interruptions.

When generating stable clonal cell lines, random vector integration could affect *FXN* transgene expression levels considerably, masking differences in *FXN* expression caused by expanded GAA repeats. For this reason, we used site-specific integration to allow controlled comparison of the two vectors. We adapted a well-described site-specific integration protocol to the BAC technology by modifying pBAC-*FXN-Luc* and pBAC-*FXN-GAA-Luc* vectors to carry a promoter-less FRT-hygromycin cassette. In the event of random vector integration in the genome, these vectors are

unable to provide hygromycin resistance; however, when co-transfected with an Flp recombinase-encoding plasmid in an acceptor cell line carrying a CMV-FRT-LacZeo construct, site-specific integration is achieved and the hygromycin cassette is expressed providing resistant clonal cell lines. FISH and copy number analysis are necessary for the generation of comparable cell lines, with one copy of the transgene and sharing the same integration site within the genome. To generate our cell model, we selected HEK-293 for their high efficiency of transfection with BAC vectors and for their ease of propagation, which makes them ideal for high-throughput screenings. We isolated two reporter clonal cell lines, *FXN-Luc* and *FXN-GAA-Luc*, and we demonstrate that the presence of $\sim$310 GAA repeats causes a reduction in FXN-luciferase mRNA and protein levels via a heterochromatin-mediated silencing mechanism. We show that the GAA expansion induces a decrease in histone acetylation and an increase in histone methylation at the promoter and at the regions upstream and downstream of the GAA repeats, in accordance with previous reports (26,27,32). Furthermore, *FXN-GAA-Luc* cells show increased CpG methylation upstream and downstream of the GAA repeat expansion when compared with *FXN-Luc* cells. Upstream of the GAA repeats, we observe increased DNA methylation at CpG sites 4 and 5, in accordance with previous data obtained using post-mortem brain and heart tissues from FRDA patients (27) and peripheral blood and buccal cells from FRDA patients (29). Our results for CpG site 6 are different from methylation data from FRDA patients (27,28) but are in agreement with data from brain tissue of FRDA mice (27). In the region downstream of the GAA repeats, we observed increased methylation at CpG sites 1, 2 and 7, whereas the rest of the CpG sites were completely methylated. Unlike our findings, analysis of methylation on cells (29) and tissues (27) from patients reported a general hypomethylation in this region. A methylation pattern similar to our findings in this region has been reported in YG8 mice, which do not present hypomethylation in this region (27). Since our results are different from the data obtained from patients, who carry large GAA expansions, but are similar to the findings in YG8 mice which carry shorter GAA repeats (190 + 90 GAA repeats), we speculate that this

change in CpG methylation could be related to the size of the GAA expansion. To explain how shorter repeat expansions cause changes in DNA methylation, Al-Mahdawi *et al.* (27) suggested that large GAA expansions increase the distance of the downstream region from a putative methylation centre at the 5′ end of the Alu sequence, located upstream of GAA repeats, thus generating hypomethylation of the region downstream of GAA repeats when compared with control individuals. However, a shorter GAA expansion would decrease such distance, thereby leading to hypermethylation in this region.

To our knowledge, this is the first GAA-expanded genomic reporter system that allows direct comparison of the effect of normal or expanded *FXN* loci on *FXN* expression. A previous *FXN* genomic reporter system has been described; however, this system does not contain expanded GAA repeats (54,55). The endogenous *FXN* gene is present in our cell model; however, detection of expression by luciferase assay and qRT-PCR targeted to the exon 5a–luciferase junction allow specific detection of transgene expression from the *FXN-Luc* and *FXN-GAA-Luc* vectors.

Cell models represent a very important tool for understanding the pathological repression of expression resulting from expanded GAA repeats and currently there are no such reporter cell models which allow direct comparison of normal and GAA-expanded genomic DNA loci. A few reporter cell models have been described so far which carry long expanded GAA repeats; however, these models do not allow the study of such repeats on *FXN* expression, since they typically carry only long GAA repeats within a reporter gene lacking any *FXN* gene sequence (31,39) or only contain a small portion of intron 1 (38). Thus, although they provide a suitable model to study GAA instability, previous models do not provide a tool to analyze how *FXN* expression is reduced in the presence of GAA repeats. Genomic DNA vectors, instead, provide the full genomic locus of a gene of interest, including the native promoter, all introns and exons and all elements necessary for regulated physiological transgene expression.

Currently, there is no proven treatment for FRDA. Future therapies are likely to be represented by combination of therapies targeting the reduced *FXN* expression, the increased oxidative stress and the intra-mitochondrial iron accumulation (36,55). However, drugs targeting the reduced *FXN* expression are the most promising strategies, since they target the primary molecular defect of FRDA. Recently, a few promising molecules have been proposed which increase *FXN* expression in patient cells (26,34,35,55). However, to increase the likelihood of developing successful treatments, it is important to increase the efficiency of discovery of such molecules. Reporter models of FRDA which reproduce the GAA-mediated *FXN* repression and the epigenetic hallmarks of FRDA represent an excellent tool to achieve this. We believe that our cell model fits these criteria and represents an excellent platform for the screening of *FXN* up-regulating compounds, since it allows high-throughput analysis of chemical libraries due to the rapid detection of FXN-luciferase expression by luciferase assay.

Here we show how the efficiency of screening can be increased by performing a pre-selection of small molecules based on their structure, since this considerably reduces the size of the primary screening. Our compound screening resulted in the identification of a novel compound which increases *FXN*

expression in FRDA patient cells by increasing histone acetylation around the GAA repeats. This finding strengthens the hypothesis that formation of highly packaged heterochromatin is involved in the transcriptional silencing induced by GAA repeats (26). C5 is a novel small molecule which shows promising potential as a therapy for FRDA as we demonstrate it achieves a consistent 1.5–2-fold *FXN* up-regulation on our cell model, on untransfected HEK cells and most importantly on primary cells from three different FRDA patients. We show in a direct side-by-side comparison a significantly greater up-regulating effect of C5 on the expanded *FXN* locus compared with the wild-type locus, demonstrating a relative specificity for GAA expansions. However, we do observe a significant increase in endogenous *FXN* expression in non-mutant HEK cells. To explain these observations, we could hypothesize that C5 affects *FXN* expression through two separate mechanisms of action, one affecting both wild-type and expanded loci and one specific to the expanded *FXN* locus. This would cause an increase in *FXN* expression in the wild-type *FXN* locus but generate a greater increase in the expanded locus. Alternatively, we could hypothesize a single mechanism of action for C5 but a different responsiveness of the expanded and the wild-type *FXN* loci, generating a different extent of up-regulation in response to C5. Regarding the extent of the *FXN* up-regulation and the specificity for the expanded *FXN* locus, C5 is comparable with other *FXN*-increasing compounds currently undergoing clinical trials, which makes C5 a promising compound. The majority of these molecules are not characterized by specificity for the expanded *FXN* locus: PPAR-γ agonists induce an ∼1.86-fold increase in *FXN* mRNA in wild-type fibroblasts and an ∼2-fold increase in FRDA primary fibroblasts (56); resveratrol elevates frataxin mRNA by 2-fold in FRDA cells and increases frataxin protein both in wild-type cells and in FRDA cells (55); erythropoietin increases frataxin protein by 1.5-fold in control individuals and by 2-fold in FRDA patients (57); nicotinamide, a class III HDAC inhibitor, up-regulates *FXN* expression in primary lymphocytes from both healthy individuals and FRDA patients, with a higher increase in expression on FRDA samples (58). The pimelic *o*-aminobenzamide HDAC inhibitors show specificity for the pathogenic *FXN* allele. The latest of such compounds show a similar or higher up-regulation of *FXN* mRNA in primary lymphocytes from patients than C5 (34,59); however, the first HDAC inhibitor identified, BML-210, induced a 2-fold up-regulation in *FXN* expression, which is comparable with the elevation induced by C5 (26).

It is worth noting that *FXN* up-regulation is the most important requirement for developing a therapy for FRDA and we do not require that a therapy for FRDA should be specific to the GAA-expanded locus. FRDA patients do not carry a wild-type allele and this implies that a compound which can successfully increase *FXN* expression but which shows less specificity for the GAA repeats is as promising as a specific one. Finally, we believe that the most likely therapeutic approach for FRDA will be a combination of therapies aimed at targeting the frataxin deficit through multiple mechanisms of action. The combined use of unspecific *FXN*-increasing compounds with molecules acting specifically on the GAA-mediated silencing may be the most promising approach to increase frataxin protein levels to those observed in asymptomatic carriers.

HDAC inhibitors are currently considered the most promising therapy for FRDA and our results suggest C5 might belong to this class of molecules, although further studies are required to identify the exact mechanism of action.

In conclusion, we have generated a novel *FXN*-reporter expression cell model which recapitulates the *FXN* gene repression seen in FRDA patients and provides a versatile tool for the dissection of the mechanism causing the *FXN* transcriptional silencing induced by expanded GAA repeats. We demonstrate one application of this tool which resulted in the identification of a promising small molecule for the therapy of FRDA. Future studies will focus on chemical modifications of C5 to generate analogues with improved activity and chemical properties.

MATERIALS AND METHODS

Ethics statement

Informed consent for participation in the study was obtained according to the Declaration of Helsinki and approved by the Central Oxford Research Ethics Committee and the Research and Development Department of the Oxford Radcliffe Hospitals NHS Trust, Oxford.

Vector construction

The BAC clone RP11-265B8 carrying the whole 80 kb *FXN* locus with exons 1 to 5b of the *FXN* gene (42) was used to generate pBAC-*FXN-Luc*. To insert the GSGSG-luciferase sequence in exon 5a, we used a selection/counter-selection homologous recombination protocol based on RedET recombination (GeneBridges, Dresden, Germany). The recombination using the RPSL-Neo and the pSC101-BAD plasmids was carried out in two steps in *Escherichia coli* according to the manufacturer's instructions. In the first step, a PCR product containing the RPSL-Neo cassette flanked by 58 bp homology arms to either side of exon 5a was used to insert the cassette in exon 5a. In the second step, the RPSL-Neo cassette was replaced with a PCR product containing the GSGSG-luciferase sequence flanked by ~155 bp homology arms. The luciferase sequence was obtained by PCR amplification on pGL3-promoter vector (Promega). Successful construction was confirmed by PCR and sequencing. To replace the ~6 GAA repeats present in pBAC-*FXN-Luc* with ~310 GAA repeats, the RPSL-Neo cassette was amplified with primers carrying 58 bp homology arms to sequences immediately upstream and downstream of GAA repeats and the product was inserted in intron 1 of pBAC-*FXN-Luc*. Subsequently, the RPSL-Neo was replaced with a PCR product containing 280 and 830 GAA repeats amplified from NA16207 using GAA-F and GAA-R primers (1). Owing to low recombination efficiency, successful recombinant bacterial colonies were identified by colony blot assay and later confirmed by Southern blot. Colony blot and Southern blot were carried out using DIG High Prime DNA Labeling and Detection Starter Kit II (Roche), according to the manufacturer's instructions and using a digoxigenin (DIG)-labelled TTC_{10} probe for detection. Sequencing of GAA repeats on the TTC strand was performed using 602R. Since sequencing of the GAA strand is blocked by the presence of a long stretch of A immediately upstream of the GAA repeats, we designed a primer called LX-1st-GAA(5′-TACTAAAAAATACAAAAAAAAAAAA-AAAAGAAG-3′) which overcomes this area and allows sequencing of the GAA strand. To test the purity of the GAA expansion, we performed a PCR of pBAC-*FXN-Luc* and pBAC-*FXN-GAA-Luc* vectors using primers GAA-F and GAA-R (1) and digested the products with *Mbo*II, according to a method described by Holloway *et al.* (46). *Cre/loxP*-mediated retrofitting of pBAC-*FXN-Luc* and pBAC-*FXN-GAA-Luc* vectors to iBAC vector and to pH-FRT-Hy was performed as previously described (40). pH-FRT-Hy was obtained by modifying pcDNA5/FRT (Life Technologies) (61). Packaging into HSV-1 amplicons was carried out as previously described (47,48).

Cell culture and primary lymphocytes

HEK-293 cells were cultured in DMEM medium supplemented with 10% fetal bovine serum (FBS), 2 mM L-glutamine, 100 U/ml penicillin/streptomycin. HEK FRT cells were generated by transfecting the pFRT-*lacZeo* plasmid (Life Technologies), followed by selection in medium containing 100 μg/ml Zeocin (Life Technologies). *FXN-GAA-Luc* and *FXN-Luc* clonal cell lines were propagated in complete DMEM medium (see above) supplemented with 100 μg/ml Hygromycin B (Life Technologies). For the CMV-Luc experiment, HEK cells were seeded in a 24-well plate at a density of 2×10^5 cells/well, and after 24 h, they were transfected with a CMV-Luc-expressing plasmid using Lipofectamine (Life Technologies) and Plus Reagent (Life Technologies). Epstein–Barr virus-transformed lymphoblastoid cell lines GM15850 (from individuals affected by FRDA, alleles with 1030 and 650 GAA repeats) and GM15851 (from an unaffected sibling with normal range of GAA repeats) were obtained from the Human Genetic Cell Repository of the Coriell Institute (USA) and propagated in RPMI1640 medium supplemented with 15% FBS and 2 mM L-glutamine. SH-SY5Y cells were cultured in DMEM/F-12 supplemented with 10% FBS, 2 mM L-glutamine, 100 U/ml penicillin/streptomycin. SH-SY5Y cells were infected with iBAC-*FXN-Luc* and iBAC-*FXN-GAA-Luc* vectors packaged in HSV-1 amplicons as previously reported (40,48). Blood was collected from anonymous individuals affected by FRDA using Vacutainer tubes. Only patients who were shown to have two expanded alleles using a PCR-based assay were included in the study. The assays were performed by accredited molecular genetic testing laboratories in the UK. Primary lymphocytes were isolated from blood samples by centrifugation on Ficoll-Paque PLUS gradient (GE Healthcare) in Leucosep tubes (Greiner Bio-One), according to the protocol described by Miltenyl Biotec. Cell viability was monitored using trypan blue exclusion and purified cells maintained in RPMI1640 medium supplemented with 15% FBS and 2 mM L-glutamine. Compounds were added to the purified cells at the concentrations indicated above and incubated for 72 h. Cells were spun down at 200*g* for 5 min at room temperature and lysed for RNA total extraction. All cells were grown at 37°C in 5% CO_2.

PCR, qPCR and copy number assay

Genomic DNA from *FXN-GAA-Luc* and *FXN-Luc* clonal cell lines was isolated by standard phenol/chloroform extraction and ethanol precipitation. PCR amplification of the GAA

repeat sequence was carried out on 200 ng of genomic DNA using primers 147F and 602R (61) and Expand Long Template DNA Polymerase (Roche) as previously described (1,45). Vector integration at the docking site was assessed by PCR analysis using primers pSV40-F (5′-CCAGTTCCGCCCATTCTC-3′) and Hygro-R (5′-CAGCTATTTACCCGCAGGAC-3′) using AmpliTaq Gold (Roche). For copy number determination, genomic DNA from *FXN-Luc* and *FXN-GAA-Luc* clonal cell lines was isolated using Illustra Tissue and Cells GenomicPrep Mini Spin Kit (GE Healthcare), according to the manufacturer's instructions. The number of transgene copies was determined by real-time PCR, using the relative standard curve method. Five-fold dilution standards were prepared to generate a standard curve for each primer pair. The upstream region of the GAA repeats in intron 1 of the *FXN* gene was amplified using the primers UpGAA-F and UpGAA-R (26) and normalizing data by GAPDH, using the primers GAPDH-F and GAPDH-R (26). Three independent genomic DNA samples per cell line were quantified in triplicate by real-time PCR using the SYBR Green PCR Master Mix (Applied Biosystems). Each 25 μl reaction contained 2 μl of genomic DNA dilution, $1 \times$ SYBR Green PCR Master Mix and 70 nM of each primer. The assay was performed using the StepOnePlus Real-Time PCR system (Applied Biosystems) with the following protocol: 10 min at 95°C for enzyme activation, followed by 40 cycles of denaturation at 95°C for 15 s and primer annealing and extension at 60°C for 1 min. Specificity of amplification was monitored with a final dissociation stage which generates a melting curve. The number of transgene copies was determined by comparison with the acceptor cell line HEK FRT as reference sample, which carries three endogenous *FXN* loci as determined by FISH.

qRT-PCR

Total RNA from HEK FRT, *FXN-Luc* and *FXN-GAA-Luc* clonal cell lines was extracted using RNeasy Mini Kit (Qiagen) and treated with RNase-Free DNase (Qiagen). cDNA was synthesized from 1 μg of total RNA using random primers (Life Technologies) and SuperScript III Reverse Transcriptase (Life Technologies) in a reaction volume of 20 μl. qPCR was carried out as described above, using qFXN-Luc-F (5′-CGG AAAAGATGCTGGAAGTG-3′) and qFXN-Luc-R (5′-AACC AGGGCGTATCTCTTCA-3′) for FXN-luciferase mRNA detection, FXN-F and FXN-R (26) for *FXN* mRNA detection, and data were normalized to GAPDH. Total RNA from primary lymphocytes was extracted and treated with DNase using RNAqueous-Micro Kit (Life Technologies). RNA was reverse-transcribed as above. *FXN* mRNA was detected using FXN-F and FXN-R (26) and data normalized to GAPDH, HPRT and Beta-Actin using the following primers: GAPDH-2F (5′-GGTCTCCTCTGACTTCAACA-3′) and GAP DH-2R (5′-AGCCAAATTCGTTGTCATAC-3′) (RTPrimer DB, ID: 912), HPRT-F (5′-GCCAGACTTTGTTGGATTT G-3′) and HPRT-R (5′-CTCTCATCTTAGGCTTTGTATTT TG-3′) (RTPrimerDB, ID: 984), ACTB-F (5′-AGCGCGGCT ACAGCTTCA-3′) and ACTB-R (5′-CGTAGCACAGCTTCT CCTTAATGTC-3′) (RTPrimerDB, ID: 2203).

Luciferase assay

FXN-GAA-Luc and *FXN-Luc* clonal cell lines were counted with trypan blue or Scepter (Millipore) and seeded in 6 cm dishes (1.5×10^6 cells/dish), 24-well (1×10^5 cells/well) or 96-well (3×10^4 cells/well) format. When assaying luciferase expression, cells were washed with PBS and lysed in Lysis Buffer (25 mM Tris−PO$_4$, pH7.8, 2 mM CDTA, 10% glycerol and 1% Triton X-100) for 20 min at 4°C. Seventy-five microlitres of lysates were mixed with 100 μl of Luciferase Assay Buffer (15 mM MgSO$_4$, 15 mM KPO$_4$, pH 7.8, 4 mM EGTA, pH 7.8, 2 mM ATP and 2 mM DTT) and 50 μl of D-Luciferin (0.3 mg/ml). The relative light units of luciferase of each cell line were determined using the Dynex MLX 96 Well Plate Luminometer and were normalized by total protein concentration, determined using Bicinchoninic acid solution (BCA, Sigma).

Compounds library and screening

The complete library is made of 25 000 compounds dissolved in DMSO at a concentration of 2.5 mg/ml. For the primary screening, *FXN-GAA-Luc* cells were seeded in 96 wells at a density of 3×10^4 cells/well and incubated in triplicate with the 88 preselected compounds at a final concentration of 20 μM for 48 h. Luciferase assay was performed as described above. An authentic sample of C5 [1-(3,4-dimethylphenoxy)-3-(4-morpholinyl)-2-propanol hydrochloride] was purchased from ChemBridge Corporation (ID: 5358626); *m/z* (ESI+) 266 (100%, [M+H]$^+$), 288 (35%, [M+Na]$^+$).

Chromatin immunoprecipitation

Analysis of histone modifications in the *FXN* promoter and regions flanking GAA repeats in lymphoblastoid (GM15850 and GM15851), *FXN-Luc* and *FXN-GAA-Luc* cell lines was performed as previously described (62). Lymphoblastoid cell lines were treated with DMSO or C5 for 48 h before cross-linking. Proteins were cross-linked to DNA by 1% formaldehyde treatment for 4 min (GM15850 and GM15851) or 7 min (*FXN-Luc* and *FXN-GAA-Luc* cells). Chromatin from lysed cells was sheared by sonication to obtain fragments from 100 to 800 bp using a Bioruptor (Diagenode). Immunoprecipitation experiments were performed using the Immunoprecipitation Kit with Dynabeads Protein G (Life Technologies), according to the manufacturer's instructions. Chromatin was incubated with one of the following antibodies at 4°C: (i) anti-H3K9ac (07−352), (ii) anti-H4K8ac (07−328), (iii) anti-H3K9me2 (07−441), (v) anti-H3K9me3 (07−442) and (vi) normal rabbit serum (12−370) used as a negative control (all antibodies were purchased from Millipore). Samples were treated with 500 mM NaCl, 0.25 mg/ml RNase A and 0.25 mg/ml proteinase K and incubated at 65°C overnight to reverse cross-linking. After reversing the cross-linking, the amount of *FXN* DNA immunoprecipitated was quantified in triplicate by real-time PCR using the SYBR Green PCR Master Mix (Applied Biosystems) and determined using the $\Delta\Delta C_t$ method. The immunoprecipitated DNA was normalized to 10% of input and taking into consideration the background signal. For the analysis of the *FXN* promoter and the regions upstream and downstream of the GAA repeats, we used primers described in Herman *et al.* (26).

Bisulfite sequencing

Genomic DNA of the *FXN-Luc* and *FXN-GAA-Luc* cell lines was isolated using the Illustra Tissue and Cells GenomicPrep Mini Spin Kit (GE Healthcare). Two micrograms of DNA was used in the bisulfite conversion reaction using the EpiTect Bisulfite kit (Qiagen), according to the manufacturer's instructions. Nested PCR was performed on bisulfite-converted DNA using HotStart Taq DNA Polymerase (Qiagen) with the following primers, described in Al-Mahdawi *et al.* (27): F1G and R1G (first-round PCR) and F2G and R2G (second-round PCR) for the upstream region of the GAA repeats in intron 1 of the *FXN* gene; NH1F and SLGR2 (first-round PCR) and NH2F and SLGR1 (second-round PCR) for the downstream region of the GAA repeats in intron 1 of the *FXN* gene. PCR products were cloned into pGEM-T easy vector. A total of 10 colonies were sequenced per region and for each cell line.

Analysis of frataxin protein

For western blot analysis of FXN-luciferase protein, *FXN-Luc* and *FXN-GAA-Luc* cells were washed in PBS and lysed in RIPA buffer (50 mM, Tris, pH 8, 150 mM NaCl, 2 mM EGTA, 0.5% sodium deoxycholate, 1% Igepal 630, 0.1% sodium dodecyl sulphate (SDS)] with protease inhibitors (Complete Mini, EDTA-free, Roche). Cell disruption was performed by repeated pipetting followed by sonication on ice (1.5 s for 10 times) (Misonix XL-2000 sonicator). Cell lysates were spun at 1300g for 15 min at 4°C, supernatant transferred to a new tube and protein concentration was determined through BCA assay. Protein samples were reduced in Laemmli buffer and incubated for 5 min at 100°C. Fifty micrograms of protein was resolved on 10% SDS−polyacrylamide gel electrophoresis (SDS−PAGE). Following transfer on a PVDF-type membrane (Immobilon P, Millipore), protein samples were incubated with the following antibodies: mouse monoclonal anti-luciferase (Santa Cruz, sc-57604, 1/1000 dilution) and rabbit polyclonal anti-Beta-Actin (Abcam, ab8227, 1/1000 dilution). Analysis of frataxin protein in HEK cells was carried out using Frataxin Dipstick Assay Kit (Mitosciences), according to the manufacturer's instructions. Protein concentration in cell lysates was quantified by BCA assay and 10 µg of total protein was loaded in each well. Dried dipsticks were imaged with Chemidoc XRS system (Bio-Rad) and quantification was performed using the Image J software.

Fluorescence *in situ* hybridization

Chromosome preparation and FISH analyses were carried out as previously described (63) using the unmodified *FXN* BAC and the plasmid pH-FRT-Hy as probes. Transgene integration on chromosome 1 was confirmed using a chromosome 1 centromeric probe.

REFERENCES

1. Campuzano, V., Montermini, L., Molto, M.D., Pianese, L., Cossee, M., Cavalcanti, F., Monros, E., Rodius, F., Duclos, F., Monticelli, A. *et al.* (1996) Friedreich's ataxia: autosomal recessive disease caused by an intronic GAA triplet repeat expansion. *Science*, **271**, 1423–1427.

2. Schulz, J.B., Boesch, S., Bürk, K., Dürr, A., Giunti, P., Mariotti, C., Pousset, F., Schöls, L., Vankan, P. and Pandolfo, M. (2009) Diagnosis and treatment of Friedreich ataxia: a European perspective. *Nat. Rev. Neurol.*, **5**, 222–234.

3. Tsou, A.Y., Paulsen, E.K., Lagedrost, S.J., Perlman, S.L., Mathews, K.D., Wilmot, G.R., Ravina, B., Koeppen, A.H. and Lynch, D.R. (2011) Mortality in Friedreich ataxia. *J. Neurol. Sci.*, **307**, 46–49.

4. Koeppen, A.H., Michael, S.C., Knutson, M.D., Haile, D.J., Qian, J., Levi, S., Santambrogio, P., Garrick, M.D. and Lamarche, J.B. (2007) The dentate nucleus in Friedreich's ataxia: the role of iron-responsive proteins. *Acta Neuropathol.*, **114**, 163–173.

5. Koeppen, A.H., Morral, J.A., Davis, A.N., Qian, J., Petrocine, S.V., Knutson, M.D., Gibson, W.M., Cusack, M.J. and Li, D. (2009) The dorsal root ganglion in Friedreich's ataxia. *Acta Neuropathol.*, **118**, 763–776.

6. Delatycki, M.B., Williamson, R. and Forrest, S.M. (2000) Friedreich ataxia: an overview. *J. Med. Genet.*, **37**, 1–8.

7. Cossée, M., Dürr, A., Schmitt, M., Dahl, N., Trouillas, P., Allinson, P., Kostrzewa, M., Nivelon-Chevallier, A., Gustavson, K.H., Kohlschütter, A. *et al.* (1999) Friedreich's ataxia: point mutations and clinical presentation of compound heterozygotes. *Ann. Neurol.*, **45**, 200–206.

8. Cossée, M., Puccio, H., Gansmuller, A., Koutnikova, H., Dierich, A., LeMeur, M., Fischbeck, K., Dollé, P. and Koenig, M. (2000) Inactivation of the Friedreich ataxia mouse gene leads to early embryonic lethality without iron accumulation. *Hum. Mol. Genet.*, **9**, 1219–1226.

9. Filla, A., De Michele, G., Cavalcanti, F., Pianese, L., Monticelli, A., Campanella, G. and Cocozza, S. (1996) The relationship between trinucleotide (GAA) repeat length and clinical features in Friedreich ataxia. *Am. J. Hum. Genet.*, **59**, 554–560.

10. Montermini, L., Richter, A., Morgan, K., Justice, C.M., Julien, D., Castellotti, B., Mercier, J., Poirier, J., Capozzoli, F., Bouchard, J.P. *et al.*

(1997) Phenotypic variability in Friedreich ataxia: role of the associated GAA triplet repeat expansion. *Ann. Neurol.*, **41**, 675–682.

11. Schmucker, S. and Puccio, H. (2010) Understanding the molecular mechanisms of Friedreich's ataxia to develop therapeutic approaches. *Hum. Mol. Genet.*, **19**, R103–R110.

12. Puccio, H., Simon, D., Cossée, M., Criqui-Filipe, P., Tiziano, F., Melki, J., Hindelang, C., Matyas, R., Rustin, P. and Koenig, M. (2001) Mouse models for Friedreich ataxia exhibit cardiomyopathy, sensory nerve defect and Fe-S enzyme deficiency followed by intramitochondrial iron deposits. *Nat. Genet.*, **27**, 181–186.

13. Martelli, A., Wattenhofer-Donzé, M., Schmucker, S., Bouvet, S., Reutenauer, L. and Puccio, H. (2007) Frataxin is essential for extramitochondrial Fe-S cluster proteins in mammalian tissues. *Hum. Mol. Genet.*, **16**, 2651–2658.

14. Babcock, M., de Silva, D., Oaks, R., Davis-Kaplan, S., Jiralerspong, S., Montermini, L., Pandolfo, M. and Kaplan, J. (1997) Regulation of mitochondrial iron accumulation by Yfh1p, a putative homolog of frataxin. *Science*, **276**, 1709–1712.

15. Rötig, A., de Lonlay, P., Chretien, D., Foury, F., Koenig, M., Sidi, D., Munnich, A. and Rustin, P. (1997) Aconitase and mitochondrial iron-sulphur protein deficiency in Friedreich ataxia. *Nat. Genet.*, **17**, 215–217.

16. Wong, A., Yang, J., Cavadini, P., Gellera, C., Lonnerdal, B., Taroni, F. and Cortopassi, G. (1999) The Friedreich's ataxia mutation confers cellular sensitivity to oxidant stress which is rescued by chelators of iron and calcium and inhibitors of apoptosis. *Hum. Mol. Genet.*, **8**, 425–430.

17. Wells, R.D. (2008) DNA triplexes and Friedreich ataxia. *FASEB J.*, **22**, 1625–1634.

18. Bidichandani, S.I., Ashizawa, T. and Patel, P.I. (1998) The GAA triplet-repeat expansion in Friedreich ataxia interferes with transcription and may be associated with an unusual DNA structure. *Am. J. Hum. Genet.*, **62**, 111–121.

19. Sakamoto, N., Chastain, P.D., Parniewski, P., Ohshima, K., Pandolfo, M., Griffith, J.D. and Wells, R.D. (1999) Sticky DNA: self-association properties of long GAA.TTC repeats in R.R.Y triplex structures from Friedreich's ataxia. *Mol. Cell*, **3**, 465–475.

20. Sakamoto, N., Ohshima, K., Montermini, L., Pandolfo, M. and Wells, R.D. (2001) Sticky DNA, a self-associated complex formed at long GAA*TTC repeats in intron 1 of the frataxin gene, inhibits transcription. *J. Biol. Chem.*, **276**, 27171–27177.

21. Grabczyk, E., Mancuso, M. and Sammarco, M.C. (2007) A persistent RNA.DNA hybrid formed by transcription of the Friedreich ataxia triplet repeat in live bacteria, and by T7 RNAP in vitro. *Nucleic Acids Res.*, **35**, 5351–5359.

22. Vetcher, A.A., Napierala, M., Iyer, R.R., Chastain, P.D., Griffith, J.D. and Wells, R.D. (2002) Sticky DNA, a long GAA.GAA.TTC triplex that is formed intramolecularly, in the sequence of intron 1 of the frataxin gene. *J. Biol. Chem.*, **277**, 39217–39227.

23. Ohshima, K., Montermini, L., Wells, R.D. and Pandolfo, M. (1998) Inhibitory effects of expanded GAA.TTC triplet repeats from intron I of the Friedreich ataxia gene on transcription and replication in vivo. *J. Biol. Chem.*, **273**, 14588–14595.

24. Grabczyk, E. and Usdin, K. (2000) The GAA*TTC triplet repeat expanded in Friedreich's ataxia impedes transcription elongation by T7 RNA polymerase in a length and supercoil dependent manner. *Nucleic Acids Res.*, **28**, 2815–2822.

25. Saveliev, A., Everett, C., Sharpe, T., Webster, Z. and Festenstein, R. (2003) DNA triplet repeats mediate heterochromatin-protein-1-sensitive variegated gene silencing. *Nature*, **422**, 909–913.

26. Herman, D., Jenssen, K., Burnett, R., Soragni, E., Perlman, S.L. and Gottesfeld, J.M. (2006) Histone deacetylase inhibitors reverse gene silencing in Friedreich's ataxia. *Nat. Chem. Biol.*, **2**, 551–558.

27. Al-Mahdawi, S., Pinto, R.M., Ismail, O., Varshney, D., Lymperi, S., Sandi, C., Trabzuni, D. and Pook, M. (2008) The Friedreich ataxia GAA repeat expansion mutation induces comparable epigenetic changes in human and transgenic mouse brain and heart tissues. *Hum. Mol. Genet.*, **17**, 735–746.

28. Greene, E., Mahishi, L., Entezam, A., Kumari, D. and Usdin, K. (2007) Repeat-induced epigenetic changes in intron 1 of the frataxin gene and its consequences in Friedreich ataxia. *Nucleic Acids Res.*, **35**, 3383–3390.

29. Evans-Galea, M.V., Carrodus, N., Rowley, S.M., Corben, L.A., Tai, G., Saffery, R., Galati, J.C., Wong, N.C., Craig, J.M., Lynch, D.R. et al. (2012) FXN methylation predicts expression and clinical outcome in Friedreich ataxia. *Ann. Neurol.*, **71**, 487–497.

30. Castaldo, I., Pinelli, M., Monticelli, A., Acquaviva, F., Giacchetti, M., Filla, A., Sacchetti, S., Keller, S., Avvedimento, V.E., Chiariotti, L. et al. (2008) DNA methylation in intron 1 of the frataxin gene is related to GAA repeat length and age of onset in Friedreich ataxia patients. *J. Med. Genet.*, **45**, 808–812.

31. Soragni, E., Herman, D., Dent, S.Y., Gottesfeld, J.M., Wells, R.D. and Napierala, M. (2008) Long intronic GAA*TTC repeats induce epigenetic changes and reporter gene silencing in a molecular model of Friedreich ataxia. *Nucleic Acids Res.*, **36**, 6056–6065.

32. Kumari, D., Biacsi, R.E. and Usdin, K. (2011) Repeat expansion affects both transcription initiation and elongation in Friedreich ataxia cells. *J. Biol. Chem.*, **286**, 4209–4215.

33. De Biase, I., Chutake, Y.K., Rindler, P.M. and Bidichandani, S.I. (2009) Epigenetic silencing in Friedreich ataxia is associated with depletion of CTCF (CCCTC-binding factor) and antisense transcription. *PLoS One*, **4**, e7914.

34. Rai, M., Soragni, E., Jenssen, K., Burnett, R., Herman, D., Coppola, G., Geschwind, D.H., Gottesfeld, J.M. and Pandolfo, M. (2008) HDAC inhibitors correct frataxin deficiency in a Friedreich ataxia mouse model. *PLoS One*, **3**, e1958.

35. Sturm, B., Stupphann, D., Kaun, C., Boesch, S., Schranzhofer, M., Wojta, J., Goldenberg, H. and Scheiber-Mojdehkar, B. (2005) Recombinant human erythropoietin: effects on frataxin expression in vitro. *Eur. J. Clin. Invest.*, **35**, 711–717.

36. Wilson, R.B. (2012) Therapeutic developments in Friedreich ataxia. *J. Child. Neurol.*, **27**, 1212–1216.

37. Velasco-Sánchez, D., Aracil, A., Montero, R., Mas, A., Jiménez, L., O'Callaghan, M., Tondo, M., Capdevila, A., Blanch, J., Artuch, R. et al. (2011) Combined therapy with idebenone and deferiprone in patients with Friedreich's ataxia. *Cerebellum*, **10**, 1–8.

38. Grant, L., Sun, J., Xu, H., Subramony, S.H., Chaires, J.B. and Hebert, M.D. (2006) Rational selection of small molecules that increase transcription through the GAA repeats found in Friedreich's ataxia. *FEBS Lett.*, **580**, 5399–5405.

39. Ditch, S., Sammarco, M.C., Banerjee, A. and Grabczyk, E. (2009) Progressive GAA.TTC repeat expansion in human cell lines. *PLoS Genet.*, **5**, e1000704.

40. Lufino, M.M., Manservigi, R. and Wade-Martins, R. (2007) An S/MAR-based infectious episomal genomic DNA expression vector provides long-term regulated functional complementation of LDLR deficiency. *Nucleic Acids Res.*, **35**, e98.

41. Wade-Martins, R., White, R.E., Kimura, H., Cook, P.R. and James, M.R. (2000) Stable correction of a genetic deficiency in human cells by an episome carrying a 115 kb genomic transgene. *Nat. Biotechnol.*, **18**, 1311–1314.

42. Gomez-Sebastian, S., Gimenez-Cassina, A., Diaz-Nido, J., Lim, F. and Wade-Martins, R. (2007) Infectious delivery and expression of a 135 kb human FRDA genomic DNA locus complements Friedreich's ataxia deficiency in human cells. *Mol. Ther.*, **15**, 248–254.

43. Puccio, H. and Koenig, M. (2000) Recent advances in the molecular pathogenesis of Friedreich ataxia. *Hum. Mol. Genet.*, **9**, 887–892.

44. Robinson, C.R. and Sauer, R.T. (1998) Optimizing the stability of single-chain proteins by linker length and composition mutagenesis. *Proc. Natl Acad. Sci. USA*, **95**, 5929–5934.

45. Al-Mahdawi, S., Pinto, R.M., Ruddle, P., Carroll, C., Webster, Z. and Pook, M. (2004) GAA repeat instability in Friedreich ataxia YAC transgenic mice. *Genomics*, **84**, 301–310.

46. Holloway, T.P., Rowley, S.M., Delatycki, M.B. and Sarsero, J.P. (2011) Detection of interruptions in the GAA trinucleotide repeat expansion in the FXN gene of Friedreich ataxia. *Biotechniques*, **50**, 182–186.

47. Wade-Martins, R., Smith, E.R., Tyminski, E., Chiocca, E.A. and Saeki, Y. (2001) An infectious transfer and expression system for genomic DNA loci in human and mouse cells. *Nat. Biotechnol.*, **19**, 1067–1070.

48. Saeki, Y., Fraefel, C., Ichikawa, T., Breakefield, X.O. and Chiocca, E.A. (2001) Improved helper virus-free packaging system for HSV amplicon vectors using an ICP27-deleted, oversized HSV-1 DNA in a bacterial artificial chromosome. *Mol. Ther.*, **3**, 591–601.

49. Westwood, I.M., Bhakta, S., Russell, A.J., Fullam, E., Anderton, M.C., Kawamura, A., Mulvaney, A.W., Vickers, R.J., Bhowruth, V., Besra, G.S. et al. (2010) Identification of arylamine N-acetyltransferase inhibitors as an approach towards novel anti-tuberculars. *Protein Cell*, **1**, 82–95.

50. Russell, A.J., Westwood, I.M., Crawford, M.H., Robinson, J., Kawamura, A., Redfield, C., Laurieri, N., Lowe, E.D., Davies, S.G. and Sim, E. (2009) Selective small molecule inhibitors of the potential breast cancer marker,

human arylamine *N*-acetyltransferase 1, and its murine homologue, mouse arylamine *N*-acetyltransferase 2. *Bioorg. Med. Chem.*, **17**, 905–918.

51. Rai, M., Soragni, E., Chou, C.J., Barnes, G., Jones, S., Rusche, J.R., Gottesfeld, J.M. and Pandolfo, M. (2010) Two new pimelic diphenylamide HDAC inhibitors induce sustained frataxin upregulation in cells from Friedreich's ataxia patients and in a mouse model. *PLoS One*, **5**, e8825.

52. Gimenez-Cassina, A., Wade-Martins, R., Gomez-Sebastian, S., Corona, J.C., Lim, F. and Diaz-Nido, J. (2011) Infectious delivery and long-term persistence of transgene expression in the brain by a 135-kb iBAC-FXN genomic DNA expression vector. *Gene Ther.*, **18**, 1015–1019.

53. Zhang, Y., Muyrers, J.P., Testa, G. and Stewart, A.F. (2000) DNA cloning by homologous recombination in *Escherichia coli*. *Nat. Biotechnol.*, **18**, 1314–1317.

54. Sarsero, J.P., Li, L., Wardan, H., Sitte, K., Williamson, R. and Ioannou, P.A. (2003) Upregulation of expression from the FRDA genomic locus for the therapy of Friedreich ataxia. *J. Gene. Med.*, **5**, 72–81.

55. Li, L., Voullaire, L., Sandi, C., Pook, M.A., Ioannou, P.A., Delatycki, M.B. and Sarsero, J.P. (2013) Pharmacological screening using an FXN-EGFP cellular genomic reporter assay for the therapy of Friedreich ataxia. *PLoS One*, **8**, e55940.

56. Marmolino, D., Acquaviva, F., Pinelli, M., Monticelli, A., Castaldo, I., Filla, A. and Cocozza, S. (2009) PPAR-gamma agonist Azelaoyl PAF increases frataxin protein and mRNA expression: new implications for the Friedreich's ataxia therapy. *Cerebellum*, **8**, 98–103.

57. Acquaviva, F., Castaldo, I., Filla, A., Giacchetti, M., Marmolino, D., Monticelli, A., Pinelli, M., Sacca, F. and Cocozza, S. (2008) Recombinant

human erythropoietin increases frataxin protein expression without increasing mRNA expression. *Cerebellum*, **7**, 360–365.

58. Chan, P.K., Torres, R., Yandim, C., Law, P.P., Khadayate, S., Mauri, M., Grosan, C., Chapman-Rothe, N., Giunti, P., Pook, M. *et al.* (2013) Heterochromatinization induced by GAA-repeat hyperexpansion in Friedreich's ataxia can be reduced upon HDAC inhibition by vitamin B3. *Hum. Mol. Genet.*, **22**, 2662–2675.

59. Soragni, E., Xu, C., Plasterer, H.L., Jacques, V., Rusche, J.R. and Gottesfeld, J.M. (2012) Rationale for the development of 2-aminobenzamide histone deacetylase inhibitors as therapeutics for Friedreich ataxia. *J. Child Neurol.*, **27**, 1164–1173.

60. Alegre-Abarrategui, J., Christian, H., Lufino, M.M.P., Mutihac, R., Venda, L.L., Ansorge, O. and Wade-Martins, R. (2009) LRRK2 regulates autophagic activity and localizes to specific membrane microdomains in a novel human genomic reporter cellular model. *Hum. Mol. Genet.*, **18**, 4022–4034.

61. Montermini, L., Andermann, E., Labuda, M., Richter, A., Pandolfo, M., Cavalcanti, F., Pianese, L., Iodice, L., Farina, G., Monticelli, A. *et al.* (1997) The Friedreich ataxia GAA triplet repeat: premutation and normal alleles. *Hum. Mol. Genet.*, **6**, 1261–1266.

62. Carey, M.F., Peterson, C.L. and Smale, S.T. (2009) Chromatin immunoprecipitation (ChIP). *Cold Spring Harb. Protoc.*, **4**, 1–8.

63. Jefferson, A. and Volpi, E.V. (2010) Fluorescence *in situ* hybridization (FISH) for genomic investigations in rat. *Methods Mol. Biol.*, **659**, 409–426.